

energy. This is shown in Figs. 4 and 8 of Reference 3 where, if the plots are renormalised with respect to the achiral case, the reflection coefficient can become greater than unity. Again, the 'real-life' nature of this work eludes us.

Although the construction of artificial dielectrics has a long history, the construction of artificial chiral media suitable for electromagnetics dates back to our work of 1979.<sup>6</sup> We are aware this construction modifies the equivalent permittivity and permeability of the composite medium.<sup>6</sup> Dr. Monzon claims that we identified the permittivity and permeability with the host material. However, this identification appears nowhere in our original paper.<sup>1</sup> Instead, we note that  $\epsilon$  and  $\mu$  are the permittivity and permeability 'of the medium'. This refers to the composite medium, not only the host medium. The fact that  $\epsilon$  and  $\mu$  are that of the composite chiral medium is also noted in the next-to-last paragraph of our original paper.<sup>1</sup> Although adding chiral microstructures to the host medium will change the equivalent  $\epsilon$  and  $\mu$  of the composite, the chiral admittance  $\xi_c$  provides an extra degree of freedom, since under certain conditions  $\xi_c$  can be changed independently.

The frequency insensitivity of the microhelices noted in our letter cannot be commented on, since the details of these structures were not specified. Methods to achieve a response which is relatively insensitive to frequency will be presented in due time. Neither we, nor any other reader of the open literature, has seen the unpublished work of Reference 4; therefore any comment here would be premature.

The comments regarding orthogonality of the field vectors deserve attention. The equations appearing in the text of Reference 1 relating electric and magnetic fields are correct, and can easily be found from the constitutive relations and the Maxwell equations. The interpretation regarding their orientations, however, holds only for the lossless case.

Eqn. 1 of the original letter<sup>1</sup> and eqn. 1 above are equivalent. However, the former is most easily connected to the accepted physical model for chiral material, and was used for that reason. Again, we reserve comment on the unpublished work.<sup>4</sup>

Although it appears that the impedance given in eqn. 2 above does not show the effect of chirality, from the physical model, we know that  $\epsilon$  and  $\mu$  given in eqns. 1 and 2 above are affected by the chirality parameter. This effect is explicitly shown in the expression given in the original paper. Therefore, we stand by our statement that chirality provides additional flexibility in tailoring RCS response by the explicit introduction of the chirality admittance  $\xi_c$ .

D. L. JAGGARD  
N. ENGHETA

14th July 1989

Moore School of Electrical Engineering  
University of Pennsylvania  
Philadelphia, PA 19104, USA

#### References

- JAGGARD, D. L., and ENGHETA, N.: 'Chirosorb™ as an invisible medium', *Electron. Lett.*, 1989, **25**, (3), pp. 173-174
- VARADAN, V. K., VARADAN, V. V., and LAKHTAKIA, A.: 'On the possibility of designing anti-reflection coatings using chiral composites', *J. Wave-Material Interaction*, 1987, **2**, pp. 71-81
- LAKHTAKIA, A., VARADAN, V. V., and VARADAN, V. K.: 'A parametric study of microwave reflection characteristics of a planar achiral-chiral interface', *IEEE Trans.*, 1986, **EMC-28**, pp. 90-95
- MONZON, J. C.: 'Radiation and scattering in homogeneous general biisotropic regions', accepted for publication in *IEEE Trans.*, AP 1985
- KONG, J. A.: 'Electromagnetic wave theory' (J. Wiley, New York, 1985)
- JAGGARD, D. L., MICKELSON, A. R., and PAPAS, C. H.: 'On electromagnetic waves in chiral media', *Appl. Phys.*, 1979, **18**, pp. 211-216

## SPICE SIMULATION OF PWM DC-DC CONVERTOR SYSTEMS: VOLTAGE FEEDBACK, CONTINUOUS INDUCTOR CONDUCTION MODE

*Indexing terms:* Circuit theory and design, Switching and switching circuits, Convertors, Simulation

A simple and straightforward method is proposed for simulating the transient and small-signal responses of open and closed-loop switch-mode DC-DC convertors. The topology-independent method hinges on the substitution of the switched inductor, fundamental in the realisation of such systems, by an equivalent circuit which represents its average behaviour. This permits simulation by a general-purpose electronic circuit simulator such as SPICE. The proposed approach is demonstrated by presenting the simulation results of a boost convertor.

**Introduction:** Switched-mode DC-DC convertors have found wide acceptance in industrial and military applications due to their high conversion efficiency and light weight. And yet the analysis and design of such systems are usually the prerogatives of the expert and highly experienced engineer. One reason for this situation is the relatively complex and formal mathematical approaches that have hitherto been suggested for the analysis and design of such systems. The mathematically rigorous approach calls for derivation of state space equations, manipulations of high-order matrices or the handling of complex transfer functions.<sup>1-3</sup> Some authors have described computer-aided analysis and design approaches, but these are based on equivalent circuits or models which have to be derived first for the system under consideration.<sup>4</sup> Other authors reported the development of specialised computer-aided analysis and design tools which, however, are a black box to the user.<sup>5-6</sup> Here I propose a simple and straightforward model that can help to translate switch mode systems into an equivalent circuit which can easily be simulated by a general purpose simulator such as SPICE.<sup>7</sup> Application of the method does not entail mathematical manipulation of

matrices or transfer functions to simulate the transient and small-signal responses of open or closed-loop switch mode systems. This letter is confined to systems with voltage feedback, operating in the inductor continuous current mode.

**Switched inductor model:** Close examination of switch-mode DC-DC convertors reveals that they all rely on a switched inductor as a temporary energy storage between input and output terminals. The fundamental switched inductor configuration (Fig. 1) covers most if not all topologies that have been described hitherto. It consists of an inductor which is switched, at one end, between two terminals (a and b in Fig. 1) at a constant frequency  $f_s$  and a duty ratio  $D$  for position a and  $D' = 1 - D$  for position b. It should be noted that physical realisations of the switched inductor may not involve the use of a toggle switch. In most topologies one of the switching branches is replaced by a stirring diode (e.g.  $D$  in Fig. 2). However, from a functional point of view the diode is in fact acting as a switch.

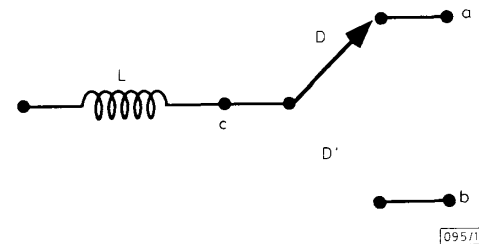


Fig. 1 Switched inductor model

The equivalent circuit of the switched inductor is easily developed by considering the average signals of the ports. Assuming an average (uninterrupted) inductor current  $I_1$  the average currents coming out of ports a and b will be  $DI_1$  and  $D'I_1$ , respectively. On the other hand, the average voltage seen into the switch is  $DV_a + D'V_b$ . This fundamental relationship leads directly to the equivalent circuit of Fig. 3 which models the average behaviour of the switched inductor. The current and voltage sources of the equivalent circuit are, for the general case, nonlinear dependent sources, i.e. their magnitude

is a product of two parameters, both of which could be variables of the systems. Fortunately, most modern SPICE versions (e.g. SPICE.2G,<sup>8</sup> PSPICE)<sup>9</sup> have a built-in capability to handle nonlinear dependent sources. They can be used both for steady-state (DC) analysis, transient analysis and small signal analysis. In the latter case the simulator first evaluates the partial derivatives of the gain function of the dependent sources around the quiescent conditions and then applies the linearised gain factors in the AC analysis. If the simulator does not include this feature one can easily derive the small-signal equivalent circuit of the switched inductor of Fig. 4. Here small letters represent averaged small signals.

The present approach differs from previous proposed methods in two main aspects: (a) it is topology-independent, as it deals only with the switched inductor in any given converter; and (b) it does not require any analytical manipulation or model transformation as a prerequisite for simulation by a general-purpose simulator. Once the switched inductor is replaced by the proposed equivalent circuit, the system is ready for simulation.

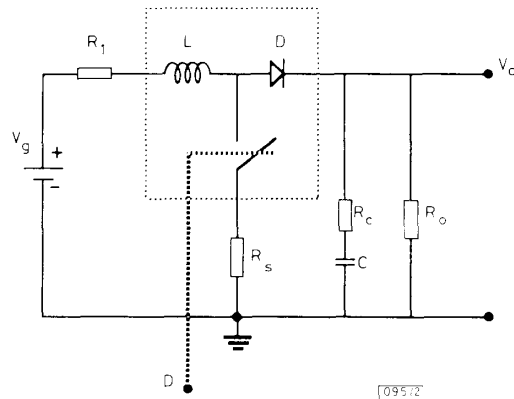


Fig. 2 Boost converter

**Results and discussions:** The proposed method was tested on a number of PWM topologies. For the sake of brevity only one specific example is presented here. The boost converter of Fig. 2 was simulated for the following component values:  $C = 5 \text{ mF}$ ,  $L = 0.45 \text{ mH}$ ,  $R_s$  (switch resistance)  $= 0.03 \Omega$ ,  $R_c = 0.01 \Omega$ ,  $R_1 = 0.4 \Omega$ ,  $V_g = 10 \text{ V}$ ,  $R_o = 118 \Omega$ . Diode parameters: SPICE.2G default values,  $D$  (duty ratio)  $= 0.8$ . Simulation of the turn-on transient and control ( $D$ ) to the output small-signal transfer function (Fig. 5) were found to be in good agreement with the results of a discrete model<sup>10</sup> (for the transient) and the average model<sup>1</sup> (for small-signal response). The simulation was carried out on GRAFSPICE developed at the Department of Electrical and Computer Engineering, Ben-Gurion University of the Negev. It is built around SPICE.2G (obtained through DECUS, Digital Equipment Co. User Group) and various service packages such as PLOT 10 (Tektronix, USA).

The transient response and the small-signal response obtainable through the simulation are averaged responses. Owing to its inherent nature the proposed equivalent circuit of the switch is incapable of describing processes within the modulation cycle or with a bandwidth close to the switching frequency  $f_s$ . This limitation is not unique to the approach

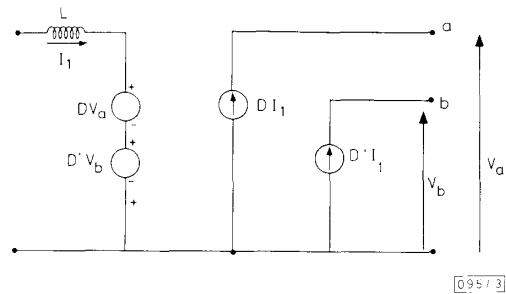


Fig. 3 Proposed equivalent circuit of switched inductor

presented here but rather to all average analysis methods discussed by many authors. However, the fact that the switching frequency in practical systems is usually much higher than the inherent frequency bandwidth of the converters, makes the average treatment a good approximation. In fact, the averaging approach is the most widely accepted one today in the practical closed-loop design of switch mode systems.<sup>11</sup> It should be pointed out that the proposed model does not take into account shifts in  $V_a$  or  $V_b$  during the switching cycle. A more rigorous analysis shows that the shifts will usually cause second-order effects in practical systems.

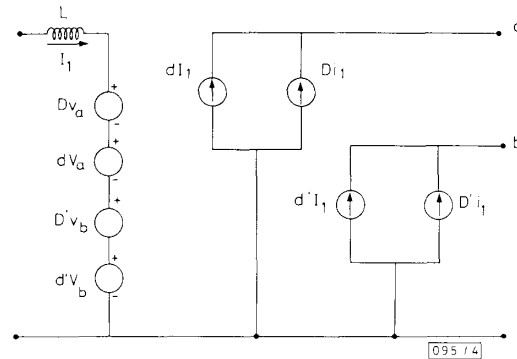


Fig. 4 Small-signal equivalent circuit of switched inductor

A major objection that can be raised against the heuristic analysis and design approach suggested here is the complete dependence on numerical analysis rather than on an analytical treatment. It is the conjecture of this author, though, that the proliferation of computer-aided tools will eventually cause a major shift in electronic analysis and design methodology toward numerical analysis and simulation. This, I believe, is a natural consequence of a basic characteristic of humans for whom one picture (Bode Plot) is often worth more than a thousand words (transfer functions or state equations).

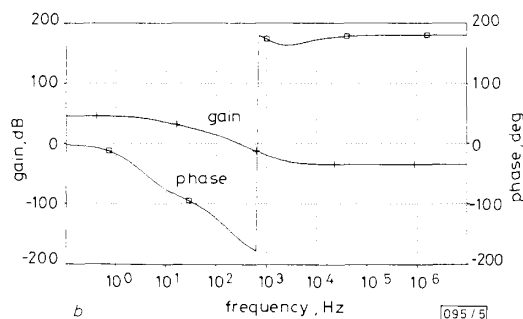
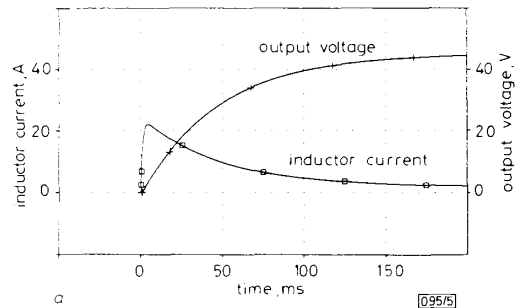


Fig. 5

a Power turn-on transient of boost converter of Fig. 2 ( $D = 0.8$ )  
 b Control to output small-signal transfer function of boost converter of Fig. 2 ( $D = 0.8$ )

**Conclusions:** The simple and straightforward model for the switched inductors presented is applicable for the electronic circuit simulation of switch-mode DC-DC converters. The proposed topology-independent approach can be used to analyse the open and closed-loop systems for transient and low-frequency small-signal response. It is further suggested that an interactive, trial-and-error simulation procedure can help to simplify and accelerate the design phase of switch-mode systems.

**Acknowledgment:** This research was supported by the Luck Hille Chair for Instrumentation Design awarded to the author. I thank my research students and in particular Mr. F. Huliehel for enthusiastic support and assistance during this SPICE adventure.

S. BEN-YAAKOV

18th May 1989

Department of Electrical & Computer Engineering  
Ben-Gurion University of the Negev  
PO Box 653, Beer-Sheva, Israel

## References

- MIDDLEBROOK, R. D., and CUK, S.: 'A general unified approach of modelling switching-converter power stages', *Int. J. Electron.*, 1977, **42**, pp. 521-550
- LEE, F. C., *et al.*: 'A unified analysis and design procedure for a standardized control for DC-DC switching regulators'. Presented at PESC-80, 1980, pp. 284-301
- MARANESI, P. G., *et al.*: 'Two port characterization of PWM voltage regulators at low frequencies', *IEEE Trans. Ind. Electron.*, 1988, **35**, pp. 444-450
- LEE, Y.-S., and CHANG, Y. C.: 'Computer-aided analysis of electronic DC-DC transformers', *IEEE Trans. Ind. Electron.*, 1988, **35**, pp. 148-152
- CUK, S., *et al.*: 'Computer aided design of switching converter frequency response'. Presented at Power CAD Conf., Los Angeles, Sept. 1987
- KELKAR, S. S., *et al.*: 'A comprehensive computer-aided design approach for switching regulators'. Presented at PESC-87, 1987
- NAGEL, L. W.: 'SPICE 2: A computer program to simulate semiconductor circuits'. Memorandum No. ERL-M520, University of California, Berkeley, 1975
- SPICE 2G: Digital Equipment Co. User Group (DECUS), Geneva, Switzerland
- PSICE: Micro Sim Co., Irvine, California
- HULIEHEL, F., and BEN-YAAKOV, S.: 'Low frequency sampled-data models of switched mode DC-DC converters'. Presented at PESC-89, Milwaukee, 26th-29th June 1989
- DIXON, L. H.: 'Closing the loop', in 'Unitrode switching regulated power supply design seminar manual' (Unitrode Co., Lexington, 1986), pp. C11-C131

## SECOND HARMONIC GENERATION BY INTERSUB-BAND TRANSITIONS IN COMPOSITIONALLY ASYMMETRICAL MQWS

*Indexing terms:* Semiconductor devices and materials, Nonlinear optics, Quantum optics, Electro-optics

We report the first experimental evidence of second harmonic generation due to intersub-band transitions in compositionally asymmetrical multi-quantum wells using a continuous CO<sub>2</sub> laser. The extremely large value of the second-order susceptibility ( $\chi_{2\omega}^{(2)} \sim 7.6 \times 10^{-7}$  m/V) is in good agreement with theoretical predictions.

Because of the quantum confinement of carriers, transitions between the sub-bands of quantum wells have an extremely large oscillator strength which may be used for mid-infrared nonlinear optics.<sup>1-3</sup> Indeed, second-order susceptibilities  $\chi_{2\omega}^{(2)}$  being proportional to the square of the oscillator strength, huge nonlinear effects are expected in so far as inversion symmetry is broken in the structure. Thus, by applying an electric field to GaAs/AlGaAs multi-quantum wells (MQW), Fejer *et al.* have obtained values of the second-harmonic generation coefficient  $\chi_{2\omega}^{(2)}$  as high as 28 nm/V, i.e. 73 times larger than

bulk GaAs.<sup>4</sup> More recently, Rosencher *et al.* have demonstrated optical rectification in compositionally asymmetrical MQWs, measuring an electro-optical coefficient  $r$  of 7.2 nm/V, i.e. more than 3 orders of magnitude higher than for bulk GaAs.<sup>5</sup> In this letter we present the first experimental evidence of second-harmonic generation by compositionally asymmetrical multi-quantum wells. The value of  $\chi_{2\omega}^{(2)}$  at 10.6  $\mu$ m is found to be  $7 \times 10^{-7}$  m/V. This huge value allows us to realise the experiment with a continuous CO<sub>2</sub> laser.

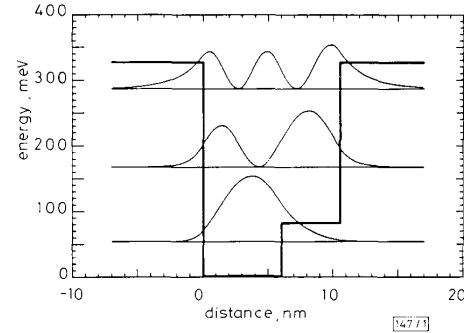


**Fig. 1** Band diagram and square of wave functions of compositionally asymmetrical quantum well used in this study

Mechanism of resonant second harmonic generation at 10.6  $\mu$ m is also symbolised by arrows

The basic idea of CA-MQW is illustrated in Fig. 1 which shows the conduction band diagram of the quantum well used in our experiment. This asymmetrical structure is experimentally realised by varying the Al composition of AlGaAs layers during growth. Let  $|i\rangle$  ( $i = 1, 2, 3$ ) be the 3 eigenstates of this potential well and  $E_i$  ( $i = 1, 2, 3$ ) the corresponding eigen-energies. The calculated energy positions and the square of the wavefunctions are also shown in Fig. 1. The structure has been optimised so that  $E_3 - E_2$  (= 119 meV) and  $E_2 - E_1$  (= 114 meV) are almost equal to the incident laser beam energy (117 meV). The second-order susceptibility  $\chi_{2\omega}^{(2)}$  is given by<sup>6</sup>

$$\chi_{2\omega}^{(2)} = \frac{q^3 n}{\epsilon_0 \hbar^2} \sum_{m,n} \langle Z_{in} \rangle \langle Z_{nm} \rangle \langle Z_{ml} \rangle \times \left\{ \frac{1}{(\omega - \Omega_{nl} - i\gamma_{nl})(2\omega - \Omega_{ml} - i\gamma_{ml})} + \frac{1}{(\omega + \Omega_{nl} - i\gamma_{nl})(2\omega + \Omega_{ml} - i\gamma_{ml})} - \frac{1}{(2\omega - \Omega_{mn} - i\gamma_{mn})} \times \left[ \frac{1}{\omega - \Omega_{ml} - i\gamma_{ml}} + \frac{1}{\omega + \Omega_{nl} - i\gamma_{nl}} \right] \right\} \quad (1)$$

where  $\langle Z_{ij} \rangle = \langle \psi_i | z | \psi_j \rangle$ ,  $\Omega_{ij} = E_i - E_j/\hbar$ ,  $1/\gamma_{ij}$  are the dephasing times, and  $q$  is the electronic charge. We assume that only the lowest level is thermally populated with a density of carriers  $n$ . It can be easily checked that this expression is nonzero only for nonsymmetric wavefunctions. Retaining the near resonant term ( $n = 2, m = 3$ ) at  $\omega \approx \Omega_{21} = \Omega_{32} = \Omega$  and  $2\omega \approx 2\Omega$  and assuming  $\gamma_{12} \approx \gamma_{31} = \gamma$ , we find

$$\chi_{2\omega}^{(2)} = \frac{q^3}{\epsilon_0 \hbar^2} n \frac{\langle Z_{12} \rangle \langle Z_{23} \rangle \langle Z_{31} \rangle}{(\omega - \Omega - i\gamma)(2\omega - 2\Omega - i\gamma)} \quad (2)$$

with a peak value for  $\omega = \Omega$  of

$$\chi_{2\omega, \max}^{(2)} = \frac{q^3}{\epsilon_0} n \frac{\langle Z_{12} \rangle \langle Z_{23} \rangle \langle Z_{31} \rangle}{(\hbar\gamma)^2} \quad (3)$$

Taking  $n = 5 \times 10^{17}$  cm<sup>-3</sup>,  $\hbar\gamma = 7$  meV,<sup>1,4-5</sup> and the dipole matrix elements given by numerical resolution of Fig. 1 [ $\langle Z_{12} \rangle = 2.1 \times 10^{-9}$  m,  $\langle Z_{23} \rangle = 3.0 \times 10^{-9}$  m and  $\langle Z_{31} \rangle = 3.8 \times 10^{-10}$  m], we find  $\chi_{2\omega, \max}^{(2)} = 8.8 \times 10^{-7}$  m/V. This is more than three orders of magnitude above the nonlinear susceptibility of GaAs ( $\chi_{2\omega}^{(2)} = 3.8 \times 10^{-10}$  m/V) and one order